Cluster Compounds

DOI: 10.1002/anie.201007332

The Dinitrogen-Ligated Triaurum Cation, Aurodiazenylium, Auronitrenium, Auroammonia, and Auroammonium**

Xinghua Liang, Xia Wu, Ting Dong, Zhengbo Qin, Kai Tan, Xin Lu, and Zichao Tang**

Gold complexes and nanoparticles exhibit fascinating properties and have found various applications recent years.[1,2] The chemistry of gold, significantly different from that of its congeners (silver and copper), is mostly dominated by its extraordinarily strong relativistic effects,[3] which impose a very small energy gap between its 5d and 6s valence orbitals and, consequently, a high degree of sd hybridization as well as an even higher electronegativity than that of the nonmetal monovalent hydrogen, that is, Au 2.54 versus H 2.20 (Pauling scale).[4] The concept of gold–hydrogen analogy thus emerged[5] and has been extensively exploited in synthetic chemistry.[1,6] Since the isolobal analogy[7] between phosphine-ligated gold ($AuPR_3$) and hydrogen (H) was noticed by Mingos[5a] in mid 1970s, the use of the $AuPR_3$ synthon has brought out to a large number of Au-containing metal cluster compounds.[1,6] Key examples are $[O(AuPPh_3)_n]^{(n-2)+}$ (n = 3,4),[8] $[N(AuPPh_3)_n]^{(n-3)+}$ (n = 4, 5),[9] $[C(AuPPh_3)_n]^{(n-4)+}$ (n = 4–6),[10] and $[N_2(AuPR_3)_6]^{2+}$,[11] which are analogous to $[OH_n]^{(n-2)+}$ (n = 3,4), $[NH_n]^{(n-3)+}$ (n = 4, 5), $[CH_n]^{(n-4)+}$ (n = 4-6), and hydrazinium $[H_3N{-}NH_3]^{2+}$, respectively. On the other hand, a simple gold–hydrogen analogy was recently observed in a series of binary Si/Au clusters $[Si_mAu_n]$ (m = 1,2; n = 2–4) in the gas phase by Wang and co-workers.[12] Herein we report a joint experimental and theoretical investigation on a series of abundant Au/N binary cluster cations, $[AuN_4]^+$, $[Au_nN_{2n+1}]^+$ (n = 2–4), and $[Au_3N_6]^+$, which exist as dinitrogen-ligated aurodiazenylium $[(N_2(AuN_2)]^+$, auronitrenium $[N(AuN_2)_2]^+$, auroammonia radical cation $[N(AuN_2)_3]^+$, auroammonium $[N(AuN_2)_4]^+$, and triaurum cation $[(AuN_2)_3]^+$, and are structurally and electronically analogous to diazenylium $([N_2H]^+)$,[13] nitrenium $([NH_2]^+)$,[14] ammonia radical cation $([NH_3]^+)$,[15] ammonium $([NH_4]^+)$, and trihydrogen cation $([H_3]^+)$,[16] respectively, by following the isolobal analogy between N_2-ligated gold (AuN_2) and hydrogen. The chemical stability of these N_2-ligated complexes suggests that they might be viable in wet chemistry. Such a N_2-assisted gold–hydrogen analogy involving a $[AuN_2]^+$ synthon and covalent dative $Au^+{-}N_2$ bond is also relevant to the industrially important nitrogen fixation.

Figure 1 displays the mass spectrum ($180 < m/e <$ 1000 amu) of $[Au_pN_q]^+$ clusters obtained by reactive collision of N_2 with laser-vaporized gold clusters. The strong mass spectral peaks for $[AuN_4]^+$, $[Au_2N_5]^+$, $[Au_3N_6]^+$, and $[Au_4N_9]^+$ indicate that these "magic-number" cations are the most abundant for the positive cluster distribution. Furthermore, the signal intensity of $[Au_3N_7]^+$, a radical cation, is comparable to that of $[Au_2N_5]^+$, likely owing to the high stability of its neutral form, Au_3N_7. Moreover, the intense signals of $[Au_mN_{(2m+1)}]^+$ (m = 2–4) with odd numbers of N atoms indicate that hot Au clusters produced by laser vaporization are capable of activating and cleaving the triple bond of the N_2 molecule.

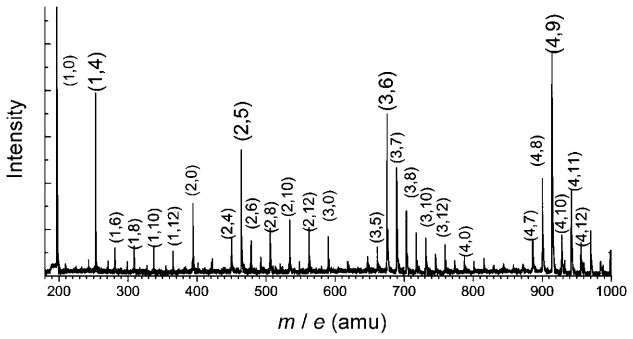

Figure 1. Mass spectrum of $[Au_pN_q]^+$ cluster cations produced by reactive collision of N_2 with laser-vaporized gold clusters. Peaks are labeled with values of p and q in parentheses as (p,q).

Density functional theory (DFT) calculations at the B3LYP/DZP level of theory (see the Supporting Information) were performed to search the ground-state structures of these abundant clusters. Figure 2 depicts the ground-state structures of these clusters re-optimized at the B3LYP/TZP level of theory.

$[AuN_4]^+$ has a linear $D_{\infty h}$-symmetric ground-state structure, $[N_2\text{-}Au\text{-}N_2]^+$ (Figure 2a), isostructural to the isoelec-

[*] X. H. Liang,[+] T. Dong,[+] Dr. K. Tan, Prof. Dr. X. Lu
State Key Laboratory of Physical Chemistry of Solid Surfaces & Fujian Provincial Key Laboratory of Theoretical and Computational Chemistry
Department of Chemistry, College of Chemistry and Chemical Engineering
Xiamen University, Xiamen 361005 (China)
Fax: (+86) 592-218-3047
E-mail: xinlu@xmu.edu.cn
X. Wu,[+] Z. B. Qin, Prof. Dr. Z. C. Tang
State Key Laboratory of Molecular Reaction Dynamics
Dalian Institute of Chemical Physics, Chinese Academy of Sciences
Dalian 116023 (China)
E-mail: zctang@dicp.ac.cn
[+] These authors contributed equally to this work.

[**] This work was supported by NSFC (Grant Nos. 20973137, 20773126, 21021061, 20923004), the Ministry of Science and Technology of China (Grant Nos. 2007CB815307 and 2011CB808504), and the Chinese Academy of Sciences.
Supporting information for this article is available on the WWW under http://dx.doi.org/10.1002/anie.201007332.

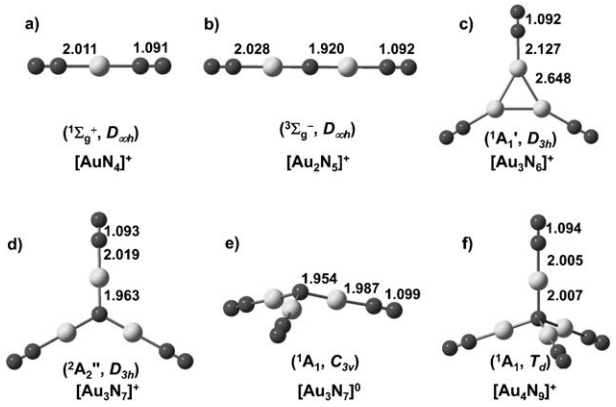

Figure 2. B3LYP/TZP-predicted ground-state structures of a) $[AuN_4]^+$, b) $[Au_2N_5]^+$, c) $[Au_3N_6]^+$, d) $[Au_3N_7]^+$, e) $[Au_3N_7]^0$, and f) $[Au_4N_9]^+$ (N black, Au gray; key bond lengths in Å).

tronic $[Au(CO)_2]^+$[17] and $[Au(CN)_2]^-$ [18a] complexes. $[Au_2N_5]^+$ has a triplet ground state $^3\Sigma_g^-$ with a linear $D_{\infty h}$-symmetric structure, $[N_2\text{-Au-N-Au-}N_2]^+$ (Figure 2b), which is 1.09 eV lower in energy than its singlet excited state, which has a C_{2v}-symmetric bent structure. Similarly, the interstellar species nitrenium $[NH_2]^+$ also has a triplet ground state ($^3B_1$) that is 2.12 eV lower than its singlet excited state.[14c]

$[Au_3N_6]^+$ has a planar D_{3h}-symmetric ground-state structure $[(AuN_2)_3]^+$ that contains a three-membered $[Au_3]^+$ ring (Figure 2c). Its Au–Au distance (2.648 Å) is slightly shorter than that of ligand-free $[Au_3]^+$ cluster (2.661 Å).[16d] Note that the central $[Au_3]^+$ unit has two skeletal valence electrons, akin to the trihydrogen cation.[16a]

$[Au_3N_7]^+$ has a $^2A_2''$ ground state with a planar D_{3h}-symmetric structure, $[N(AuN_2)_3]^+$ (Figure 2d). The neutral molecule $N(AuN_2)_3$ has a closed-shell singlet ground state with a C_{3v}-symmetric structure (Figure 2e). A similar structural change was found from $[NH_3]^+$ (D_{3h}) to NH_3 (C_{3v}).[15] $[Au_4N_9]^+$ has a T_d-symmetric ground-state structure $[N(AuN_2)_4]^+$ (Figure 2f), analogous to $[NH_4]^+$ and $[N(AuPPh_3)_4]^+$.[9]

As discussed above, the ground states of these Au/N binary clusters exhibit two structural features. First, all Au atoms in these clusters (except in $[(AuN_2)_3]^+$) are bi-coordinated. Second, they have a N_2-ligated central moiety X, $X = N_nAu_m^+$ ($n=0$, $m=3$; $n=1$, $m=2$–4; $n=2$, $m=1$), that is isostructural to the corresponding interstellar species $N_nH_m^+$ ($n=0$, $m=3$; $n=1$, $m=2$–4; $n=2$, $m=1$), implying a N_2-assisted gold–hydrogen analogy. Such a N_2-assisted gold–hydrogen analogy involves a N_2-ligated Au atom (i.e., AuN_2) as synthon, which is in effect similar to the widely exploited $AuPR_3$ synthon.[1,5] We will demonstrate such N_2-assisted gold–hydrogen analogy by analyzing the Au–N_2 bonding and by comparing the molecular orbitals (MOs) of these Au/N binary clusters with their N/H analogues.

We first consider the Au–N_2 bonding in $[Au(N_2)_2]^+$. The DFT-predicted Au^+–N_2 binding energy increases from 0.98 eV in $[AuN_2]^+$ to 1.17 eV in $[Au(N_2)_2]^+$. Further addition of a N_2 molecule to $[Au(N_2)_2]^+$ results in a van der Waals complex, with the third N_2 being weakly bound (see the Supporting Information). It is clear that Au^+ prefers a linear bi-coordinate environment, and the resultant Au^+–N_2 dative bond is covalent in nature.

The Au^+–N_2 bonding can be understood by using the Dewar–Chatt–Duncanson complexation model.[19] As shown in Figure 3, the 6σ MO in $[AuN_2]^+$ and the $5\sigma_g$ MO in $[Au(N_2)_2]^+$ account for the Au^+–N_2 σ bonding donation, whereas the 3π MOs in $[AuN_2]^+$ and the $2\pi_g$ MOs in

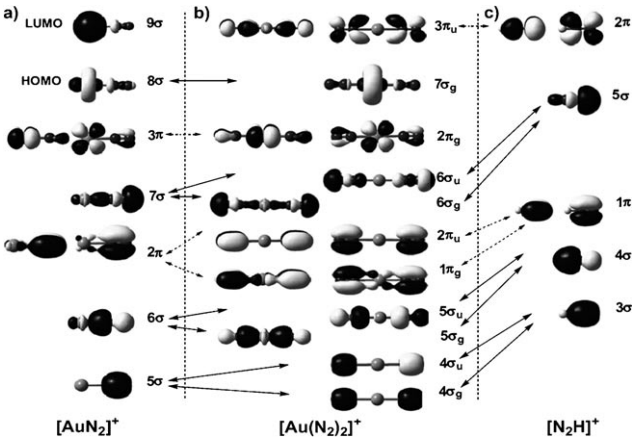

Figure 3. Selected valence orbitals (isosurface value ca. 0.04) of a) $[AuN_2]^+$, b) $[Au(N_2)_2]^+$, and c) $[N_2H]^+$. Solid and dash arrows indicate the correlation of σ- and π-type MOs, respectively, between them.

$[Au(N_2)_2]^+$ account for the Au^+–N_2 π bonding back-donation. Yet, further NBO analyses revealed that the Au^+–N_2 bonding is dominated by σ bonding donation with marginal contribution from π bonding back-donation, as the estimated σ donation and π back-donation is 0.12 e and 0.06 e in $[AuN_2]^+$ and 0.21 e and 0.07 e per N_2 in $[Au(N_2)_2]^+$. The higher degree of σ donation in $[Au(N_2)_2]^+$ is a result of enhanced sd_σ hybridization of bi-coordinated Au (see the Supporting Information). For the same reason, even stronger and shorter Au^+–ligand bonding was previously found in $[Au(CO)_2]^+$ and $[Au(CN)_2]^-$ complexes.[17,18]

Besides $[Au(N_2)_2]^+$, other abundant Au/N binary clusters (now represented by the general formula $X(N_2)_n$) have similar Au–N_2 covalent dative bonds. As listed in Table 1, the average Au–N_2 binding energy ranges from 0.57 eV in

Table 1: B3LYP/TZP-predicted Wiberg bond order (WBO) and average binding energy E_{av} of Au–N_2 bond(s) in the $X(N_2)_n$ clusters (X = central moiety) and their HOMO–LUMO gap E_g.

$X(N_2)_n$	X	WBO	E_{av}[a] [eV]	E_g[b] [eV]
$[AuN_2]^+$	Au^+	0.30	0.98 (0.95)[c]	4.91 (4.37)
$[Au(N_2)_2]^+$	$[N_2Au]^+$	0.40	1.36 (1.42)[c]	6.77 (4.91)
$[(AuN_2)_3]^+$	$[Au_3]^+$	0.24	0.57	5.54 (3.79)
$[N(AuN_2)_2]^+$	$[NAu_2]^+$	0.36	1.12	1.09 (0.75)[d]
$[N(AuN_2)_3]^+$	$[NAu_3]^+$	0.38	1.05	–
$[N(AuN_2)_3]^0$	$[NAu_3]^0$	0.42	0.72	3.64 (3.07)
$[N(AuN_2)_4]^+$	$[NAu_4]^+$	0.40	1.04	5.19 (2.57)

[a] $E_{av}(Au-N_2) = \{E(X) + nE(N_2) - E[X(N_2)_n]\}/n$; [b] The E_g of central X moiety is given in parenthesis. [c] The CCSD(T)/TZP-predicted E_{av} is given in parenthesis. [d] The energy gap between the triplet ground state and the singlet excited state.

$[(AuN_2)_3]^+$ to 1.12 eV in $[N(AuN_2)_2]^+$, and the Au–N_2 bond order is between 0.24 in $[(AuN_2)_3]^+$ and 0.42 in $[N(AuN_2)_3]^0$. Moreover, the gap between the highest occupied and lowest unoccupied MOs (HOMO–LUMO gap) of the $X(N_2)_n$ clusters is generally larger than that of the corresponding ligand-free X clusters, for example, 5.54 eV for $[(AuN_2)_3]^+$ versus 3.79 eV for $[Au_3]^+$ and 5.19 eV for $[N(AuN_2)_4]^+$ versus 2.57 eV for $[NAu_4]^+$ (Table 1). Thus, ligation of N_2 molecules to the X species enhances not only their thermal stability but also their kinetic stability. That is why a N_2-assisted gold–hydrogen analogy, but not the simple gold–hydrogen analogy, is observed in the Au/N binary clusters.

Underlying the N_2-assisted gold–hydrogen analogy is the isolobal analogy between the $[AuN_2]^+$ synthon and H^+. Indeed, the LUMO (i.e., 9σ MO) of $[AuN_2]^+$ (Figure 3a) is dominated by the Au 6s orbital, analogous to the empty 1s orbital of H^+. By following the $[AuN_2]^+$–H^+ isolobal analogy, it is $[Au(N_2)_2]^+$, rather than $[AuN_2^+]$, that is equivalent to $[N_2H]^+$. As shown in Figure 3, while the occupied valence orbitals of $[N_2H]^+$ can find their equivalence in $[AuN_2]^+$ and $[Au(N_2)_2]^+$, its π-type LUMOs (i.e., the $2\pi^*$ antibonding orbitals of the N_2 moiety) are akin to the π-type LUMOs of $[Au(N_2)_2]^+$ but strikingly different from the σ-type LUMO of $[AuN_2]^+$.

Figure 4 shows the skeletal valence orbitals of $[(AuN_2)_3]^+$, $[Au_3]^+$, and $[H_3]^+$, consisting primarily of the 6s/1s-orbitals of the ring Au/H atoms. The resemblance in skeletal valence orbitals of these clusters gives evidence of the isolobal

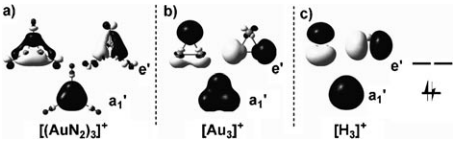

Figure 4. Skeletal valence orbitals (isosurface value ca. 0.04) of a) $[(AuN_2)_3]^+$, b) $[Au_3]^+$, and c) $[H_3]^+$.

$[AuN_2]^+$–H^+ analogy as well as the simple Au–H analogy. The diatomic Wiberg bond order is 0.39 for Au–Au in $[(AuN_2)_3]^+$, close to that of $[H_3]^+$ (0.44); $[Au_3]^+$ has a slightly larger Au–Au bond order of 0.52. Moreover, all three of these species have an in-plane three-center-two-electron (3c-2e) bond (i.e., the occupied a' MO) that conforms to the Hückel rule of aromaticity. Consequently, they are σ-aromatic with predicted NICS values of $\delta = -42.8$, -33.4, and -33.8 ppm for $[(AuN_2)_3]^+$, $[Au_3]^+$, and $[H_3]^+$, respectively.

Figure 5 shows the selected valence orbitals of the $[NR_2]^+$, NR_3, and $[NR_4]^+$ series of clusters (R = AuN_2, Au and H). These N-centered valence MOs are mainly composed of the valence 2s and 2p atomic orbitals of the central N atom and the 6s/1s orbitals of the surrounding Au/H atoms, except for the substantial sd-hybridization in Au. For each of the species, such N-centered MOs jointly account for its N–R covalent bonds and, if available, the lone-pair (or unpaired for the $[NR_2]^+$ series) electrons localized on the central N atom. For each series of species, the resemblance in the N-centered valence orbitals is terrific, evidencing the isolobal $[AuN_2]^+$–H^+ analogy and the simple Au–H analogy. The computed N–

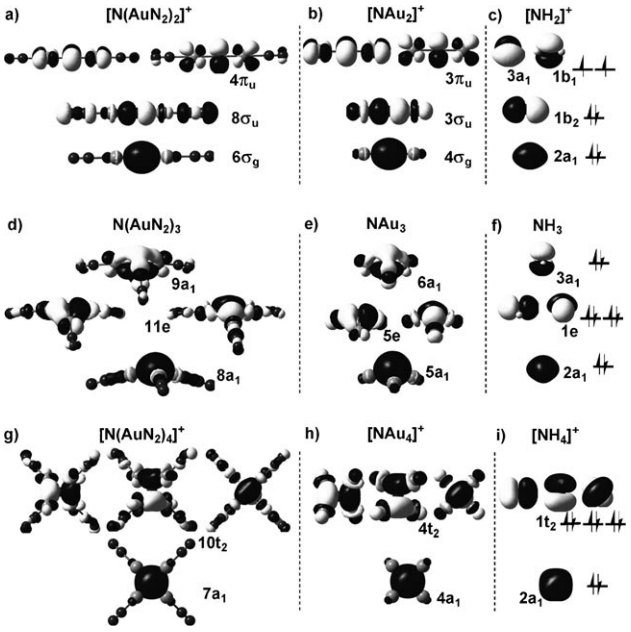

Figure 5. N-centered valence orbitals of $[NR_2]^+$, NR_3, and $[NR_4]^+$ (R = AuN_2, Au, and H).

Table 2: B3LYP/TZP-predicted Wiberg bond order of N–R bond(s) in the $[NR_2]^+$, NR_3, and $[NR_4]^+$ series of species (R = H, Au, and AuN_2).

	R = H	R = Au	R = AuN_2
$[NR_2]^+$	0.79	0.68	0.64
NR_3	0.88	0.85	0.59
$[NR_4]^+$	0.79	0.56	0.46

R bond orders are listed in Table 2. For R = Au or AuN_2, the computed N–R bond order ranges from 0.46 in $[N(AuN_2)_4]^+$ to 0.85 in $N(AuN_2)_3$, showing the covalent nature of the N–R bonds. Although the N–(AuN_2) bond in $[N(AuN_2)_4]^+$ is the weakest, the loss of $[AuN_2]^+$ shown in Equation (1) is found to be highly endothermic by 4.32 eV, thus confirming the strong covalency of the N–(AuN_2) bond.

$$[N(AuN_2)_4]^+ \rightarrow N(AuN_2)_3 + [AuN_2]^+ \qquad \Delta E = 4.32\ \text{eV} \qquad (1)$$

The ionization potential of N_2-ligated auroammonia N-$(AuN_2)_3$ is predicted to be 6.62 eV, which is 3.57 eV lower than that of ammonia. Therefore, $N(AuN_2)_3$ is much more electron-donating and could be a better ligand than ammonia.

In conclusion, we have shown that a N_2-assisted gold–hydrogen analogy, that is, the isolobal analogy between $[AuN_2]^+$ and H^+, underlies the remarkable chemical stability of a series of abundant Au/N binary cations ($[AuN_4]^+$, $[Au_nN_{2n+1}]^+$ (n = 2–4), and $[Au_3N_6]^+$) produced by laser vaporization. We are looking forward to wet-chemistry synthesis[34] of these N_2-ligated auroammonia and auroammonium species and the σ-aromatic $[(AuN_2)_3]^+$ complex. Such a dinitrogen-assisted gold–hydrogen analogy with involvement of a $[AuN_2]^+$ synthon and the relatively inert N_2 ligand opens a new way for exploring the chemistry of gold by either gas-phase dry chemistry or bench chemistry.

Experimental Section

Mass spectrometry: The experiments were carried out using a reflection time-of-flight mass spectrometer (RTOF) with a laser vaporization cluster source.[20] A vaporization laser beam (532 nm, Nd:YAG laser, about 5–10 mJ per pulse) was focused on the rotated gold target disk. The resulting ablation plasma plume crossed and was carried downstream by expanding 3–10 atm of a nitrogen gas packer from the pulsed valve. The positive ions were extracted by a high-voltage pulse (about 1.2 kV) and subjected to RTOF.[21] The mass spectrum signals of RTOF were detected by a microchannel plate (MCP) detector. The total length of the flight tubes of RTOF is about 2.2 m, with a mass resolution better than 2800.

Theoretical calculations: All quantum chemical calculations were carried out using Gaussian03.[22] Geometry optimizations of various possible isomers of the Au/N binary clusters were performed using the hybrid density functional B3LYP[23] in combination with double-ξ basis set plus polarization (DZP), that is, the standard 6-31G* basis set[24] for N and Stuttgart/Dresden relativistic effective core potential plus valence double-ξ basis set (SDD)[25] for Au. The as-determined ground-state structures were re-optimized at the B3LYP/TZP level, in which TZP refers to Aug-cc-pVTZ basis set[26] for N and H as well as the scalar-relativistic effective 60-electron core potential[27] plus the 19-electron valence aug-cc-pVTZ-PP basis set[28] for Au. Vibrational frequencies were computed to characterize the nature of the stationary points and to get the zero-point energy (ZPE). Basis set superposition error (BSSE) was estimated by using the counterpoise method.[29] The natural bond orbital (NBO) method[30] was used for bonding analyses. Single-point CCSD(T)[31] calculations using the B3LYP-optimized geometries were performed for $[Au(N_2)_n]^+$ ($n = 1$–3) to justify the B3LYP-predicted Au^+–N_2 binding energy. Unless otherwise specified, reported binding energies are ZPE- and BSSE-corrected. The NICS (nucleus-independent chemical shift)[32] values were computed using the GIAO method[33] at the B3LYP/TZP level.

Received: November 22, 2010
Published online: February 1, 2011

Keywords: density functional calculations · gold · isolobal relationship · mass spectrometry · nitrogen

[1] a) G. J. Hutchings, M. Brust, H. Schmidbaur, *Chem. Soc. Rev.* **2008**, *37*, 1759–1765; b) R. A. Sperling, P. Rivera Gil, F. Zhang, M. Zanella, W. J. Parak, *Chem. Soc. Rev.* **2008**, *37*, 1896–1908; c) V. W.-W. Yam, E. C.-C. Cheng, *Chem. Soc. Rev.* **2008**, *37*, 1806–1813; d) M. C. Gimeno, A. Laguna, *Chem. Soc. Rev.* **2008**, *37*, 1952–1966.

[2] a) J. F. Li, Y. F. Huang, Y. Ding, Z. L. Yang, S. B. Li, X. S. Zhou, F. R. Fan, W. Zhang, Z. Y. Zhou, D. Y. Wu, B. Ren, Z. L. Wang, Z. Q. Tian, *Nature* **2010**, *464*, 392–395; b) N. J. Baxter, A. M. Hounslow, M. W. Bowler, N. H. Williams, G. M. Blackburn, J. P. Waltho, *J. Am. Chem. Soc.* **2009**, *131*, 16334–16335.

[3] a) J. P. Desclaux, P. Pyykkö, *Chem. Phys. Lett.* **1976**, *39*, 300–303; b) P. Pyykkö, *Chem. Rev.* **1988**, *88*, 563–594; c) P. Schwerdtfeger, *Heteroat. Chem.* **2002**, *13*, 578–584; d) H. Schwarz, *Angew. Chem.* **2003**, *115*, 4580–4593; *Angew. Chem. Int. Ed.* **2003**, *42*, 4442–4454; e) H. Schmidbaur, S. Cronje, B. Djordjevic, O. Schuster, *Chem. Phys.* **2005**, *311*, 151–161; f) W. Huang, M. Ji, C.-D. Dong, X. Gu, L.-M. Wang, X. G. Gong, L.-S. Wang, *Acs Nano* **2008**, *2*, 897–904.

[4] a) A. L. Allred, *J. Inorg. Nucl. Chem.* **1961**, *17*, 215–221; b) P. Schwerdtfeger, *Chem. Phys. Lett.* **1991**, *183*, 457–463.

[5] a) D. M. P. Mingos, *J. Chem. Soc. Dalton Trans.* **1976**, 1163–1169; b) D. G. Evans, D. M. P. Mingos, *J. Organomet. Chem.* **1982**, *232*, 171–191; c) J. W. Lauher, K. Wald, *J. Am. Chem. Soc.* **1981**, *103*, 7648–7650.

[6] a) C. E. Briant, B. R. C. Theobald, J. W. White, L. K. Bell, A. J. Welch, D. M. P. Mingos, *J. Chem. Soc. Chem. Commun.* **1981**, 201–202; b) D. M. P. Mingos, *Pure Appl. Chem.* **1980**, *52*, 705–712; c) K. P. Hall, D. M. P. Mingos, *Prog. Inorg. Chem.* **1984**, *32*, 237–254.

[7] R. Hoffmann, *Angew. Chem.* **1982**, *94*, 725–739; *Angew. Chem. Int. Ed. Engl.* **1982**, *21*, 711–724.

[8] a) A. N. Nesmeyanov, K. I. Grandberg, V. P. Dyadchenko, D. A. Lemenovskii, E. G. Perevalova, *Izv. Akad. Nauk SSSR Ser. Khim.* **1974**, 740; b) H. Schmidbaur, S. Hofreiter, M. Paul, *Nature* **1995**, *377*, 503–504.

[9] a) Y. L. Slovokhotov, Y. T. Struchkov, *J. Organomet. Chem.* **1984**, *277*, 143–146; b) A. Grohmann, J. Riede, H. Schmidbaur, *Nature* **1990**, *345*, 140–142; c) E. Zeller, H. Beruda, A. Kolb, P. Bissinger, J. Riede, H. Schmidbaur, *Nature* **1991**, *352*, 141–143.

[10] a) F. Scherbaum, B. Huber, G. Müller, H. Schmidbaur, *Angew. Chem.* **1988**, *100*, 1600–1602; *Angew. Chem. Int. Ed. Engl.* **1988**, *27*, 1542–1544; b) F. Scherbaum, A. Grohmann, G. Müller, H. Schmidbaur, *Angew. Chem.* **1989**, *101*, 464–466; *Angew. Chem. Int. Ed. Engl.* **1989**, *28*, 463–465; c) H. Schmidbaur, O. Steigelmann, *Z. Naturforsch. B* **1992**, *47*, 1721–1724.

[11] H. Shan, Y. Yang, A. J. James, P. R. Sharp, *Science* **1997**, *275*, 1460–1462.

[12] a) B. Kiran, X. Li, H. J. Zhai, L. F. Cui, L. S. Wang, *Angew. Chem.* **2004**, *116*, 2177–2181; *Angew. Chem. Int. Ed.* **2004**, *43*, 2125–2129; b) X. Li, B. Kiran, L. S. Wang, *J. Phys. Chem. A* **2005**, *109*, 4366–4374.

[13] a) B. E. Turner, *Astrophys. J.* **1974**, *193*, L83; b) S. Green, J. Montgomery, P. Thaddeus, *Astrophys. J.* **1974**, *193*, L89; c) K. C. Sears, J. W. Ferguson, T. J. Dudley, R. S. Houk, M. S. Gordon, *J. phys. Chem. A* **2008**, *112*, 2610–2617.

[14] a) E. Herbst, W. Klemperer, *Astrophys. J.* **1973**, *185*, 505–533; b) Y. Kabbadj, T. R. Huet, D. Uy, T. Oka, *J. Mol. Spectrosc.* **1996**, *175*, 277–288; c) J. C. Stephens, Y. Yamaguchi, C. D. Sherrill, H. F. Schaeffer, *J. Phys. Chem. A* **1998**, *102*, 3999–4006; d) G. I. Borodkin, V. G. Shubin, *Russ. Chem. Rev.* **2008**, *77*, 395–419.

[15] D. C. Frost, C. A. McDowell, D. A. Vroom, *Can. J. Chem.* **1967**, *45*, 1343–1346.

[16] a) T. Oka, *Proc. Natl. Acad. Sci. USA* **2006**, *103*, 12235–12242; b) R. W. A. Havenith, F. De Proft, P. W. Fowler, P. Geerlings, *Chem. Phys. Lett.* **2005**, *407*, 391–396; c) G. D. Carney, R. N. Porter, *J. Chem. Phys.* **1976**, *65*, 3547–3565; for theoretical work on $[Au_3]^+$, see: d) R. Wesendrup, T. Hunt, P. Schwerdtfeger, *J. Chem. Phys.* **2000**, *112*, 9356–9362.

[17] a) K. Mogi, Y. Sakai, T. Sonoda, Q. Xu, Y. Souma, *J. Phys. Chem. A* **2003**, *107*, 3812–3821; b) J. Velasquez, B. Njegic, M. S. Gordon, M. A. Duncan, *J. Phys. Chem. A* **2008**, *112*, 1907–1913.

[18] a) X. B. Wang, Y. L. Wang, J. Yang, X. P. Xing, J. Li, L. S. Wang, *J. Am. Chem. Soc.* **2009**, *131*, 16368–16370; b) P. Zaleski-Ejgierd, M. Patzschke, P. Pyykkö, *J. Chem. Phys.* **2008**, *128*, 224303.

[19] a) J. Chatt, G. A. Rowe, A. A. Williams, *Proc. Chem. Soc. London* **1957**, 208; b) J. Chatt, L. A. Duncanson, R. G. Guy, *J. Chem. Soc.* **1961**, 827.

[20] X. Wu, Z. Qin, H. Xie, X. Wu, R. Cong, Z. Tang, *Chin. J. Chem. Phys.* **2010**, *23*, 373–380.

[21] W. C. Wiley, I. H. McLaren, *Rev. Sci. Instrum.* **1955**, *26*, 1150–1157.

[22] Gaussian 03 (Rev. E 01). M. J. Frisch et al., Gaussian, Inc., Wallingford CT, **2004** (see the Supporting Information).

[23] a) A. D. Becke, *J. Chem. Phys.* **1993**, *98*, 5648–5652; b) C. Lee, W. Yang, R. G. Parr, *Phys. Rev. B* **1988**, *37*, 785–789.

[24] W. J. Hehre, R. Ditchfield, J. A. Pople, *J. Chem. Phys.* **1972**, *56*, 2257–2261.

[25] D. Andrae, U. Haeussermann, M. Dolg, H. Stoll, H. Preuss, *Theor. Chem. Acc.* **1990**, *77*, 123–141.

[26] R. A. Kendall, T. H. Dunning, R. J. Harrison, *J. Chem. Phys.* **1992**, *96*, 6796 – 6806.
[27] D. Figgen, G. Rauhut, M. Dolg, H. Stoll, *Chem. Phys.* **2005**, *311*, 227 – 244.
[28] K. A. Peterson, C. Puzzarini, *Theor. Chem. Acc.* **2005**, *114*, 283 – 296.
[29] S. F. Boys, F. Bernardi, *Mol. Phys.* **1970**, *19*, 553 – 566.
[30] A. E. Reed, L. A. Curtiss, F. Weinhold, *Chem. Rev.* **1988**, *88*, 899 – 926.
[31] a) G. D. Purvis, R. J. Bartlett, *J. Chem. Phys.* **1982**, *76*, 1910 – 1918; b) C. Hampel, K. A. Peterson, H.-J. Werner, *Chem. Phys. Lett.* **1992**, *190*, 1 – 12; c) P. J. Knowles, C. Hampel, H.-J. Werner, *J. Chem. Phys.* **1993**, *99*, 5219 – 5227.
[32] a) Z. Chen, C. S. Wannere, C. Corminboeuf, R. Puchta, P. von R. Schleyer, *Chem. Rev.* **2005**, *105*, 3842 – 3888; b) P. von R. Schleyer, C. Maerker, A. Dransfeld, H. J. Jiao, N. J. R. v. E. Hommes, *J. Am. Chem. Soc.* **1996**, *118*, 6317 – 6318.
[33] K. Wolinski, J. F. Hilton, P. J. Pulay, *J. Am. Chem. Soc.* **1990**, *112*, 8251 – 8260.
[34] For rational synthesis of gold azide species, see: a) W. Beck, T. M. Klapötke, P. Klüfers, G. Kramer, C. M. Rienäcker, *Z. Anorg. Allg. Chem.* **2001**, *627*, 1669 – 1674; b) T. M. Klapötke, B. Krumm, J.-C. Galvez-Ruiz, H. Nöth, *Inorg. Chem.* **2005**, *44*, 9625 – 9627.

